Phytopathology • 2018 • 108:299-307 • https://doi.org/10.1094/PHYTO-05-17-0190-R

Virology

e-Xtra*

Identification of a Hypervirulent Pathotype of *Rice yellow mottle virus*: A Threat to Genetic Resistance Deployment in West-Central Africa

Eugénie Hébrard,† Agnès Pinel-Galzi, Aderonke Oludare, Nils Poulicard, Jamel Aribi, Sandrine Fabre, Souley Issaka, Cédric Mariac, Alexis Dereeper, Laurence Albar, Drissa Silué, and Denis Fargette

First, second, fourth, fifth, sixth, ninth, eleventh, and twelfth authors: IRD, Cirad, Université Montpellier, IPME, Montpellier, France; third author: AfricaRice Center, 01 BP 2551, Bouaké 01, Côte d'Ivoire; seventh author: FSAE, Université de Tillabéri, BP 175 Tillabéri, Niger; and eighth and tenth authors: IRD, Université Montpellier, DIADE, Montpellier, France.
Accepted for publication 4 October 2017.

ABSTRACT

Rice yellow mottle virus (RYMV) causes high losses to rice production in Africa. Several sources of varietal high resistance are available but the emergence of virulent pathotypes that are able to overcome one or two resistance alleles can sometimes occur. Both resistance spectra and viral adaptability have to be taken into account to develop sustainable rice breeding strategies against RYMV. In this study, we extended previous resistance spectrum analyses by testing the *rymv1-4* and *rymv1-5* alleles that are carried by the rice accessions Tog5438 and Tog5674, respectively, against isolates that are representative of RYMV genetic and pathogenic diversity. Our study revealed a hypervirulent pathotype, named thereafter pathotype T′, that is able to overcome all known sources of high resistance. This pathotype, which is spatially localized in West-Central Africa, appears to be more abundant than previously suspected. To better understand the adaptive processes of pathotype T′, molecular determinants of resistance breakdown were identified via Sanger sequencing and validated through directed mutagenesis of an infectious clone. These analyses confirmed the key role of convergent nonsynonymous substitutions in the central part of the viral genome-linked protein to overcome *RYMV1*-mediated resistance. In addition, deep-sequencing analyses revealed that resistance breakdown does not always coincide with fixed mutations. Actually, virulence mutations that are present in a small proportion of the virus population can be sufficient for resistance breakdown. Considering the spatial distribution of RYMV strains in Africa and their ability to overcome the *RYMV* resistance genes and alleles, we established a resistance-breaking risk map to optimize strategies for the deployment of sustainable and resistant rice lines in Africa.

First reported 50 years ago, *Rice yellow mottle virus* (RYMV) is a major biotic constraint to rice cultivation in Africa (Séré et al. 2013). RYMV is a viral species of genus *Sobemovirus* that is responsible for high rice production losses in agroecosystems in most rice-growing countries of Africa (Kouassi et al. 2005; Traoré et al. 2015). Highly adapted to the two cultivated rice species, Asian rice *Oryza sativa* and African rice *O. glaberrima*, RYMV has a narrow host range that also includes other wild *Poaceae* species (Bakker 1974). RYMV possesses a single-stranded RNA genome that is organized into five open reading frames (ORF) (Fig. 1A). Highly diverse, RYMV is classified into six major strains with a strong geographical distribution. Strains S1 and S2/S3 are found in West and West-Central Africa whereas strains S4, S5, and S6 are present exclusively in East Africa (Pinel-Galzi et al. 2015). This spatial pattern of RYMV diversity is explained by the absence of seedborne transmission and of long-distance movement (Allarangaye et al. 2006; Fargette et al. 2006; Konaté et al. 2001). In addition to short-distance propagation that is mainly mediated by beetles, RYMV is transmitted by contact during agricultural practices such as transplantation from rice nurseries to fields (Bakker 1974; Traoré et al. 2006b).

†Corresponding author: E. Hébrard; E-mail: eugenie.hebrard@ird.fr

This work was supported financially by the Global Rice Science Partnership (GRiSP) as a New Frontiers Research program (project MENERGEP) and by the French National Research Agency as an "Investissements d'avenir" program (ANR-10-LABX-001-01 Labex Agro) and was coordinated by the Agropolis Foundation (projects number1403-066 SURVEY and number 1504-004 E-SPACE).

*The *e-Xtra* logo stands for "electronic extra" and indicates that one supplementary figure and six supplementary tables are published online.

In combination with the surveillance of seedbed contamination (Traoré et al. 2006b), varietal selection is the most efficient and sustainable way to manage RYMV. Several sources of resistance have been identified in the two cultivated rice species. Only two among the thousands of *O. sativa* tested accessions are highly resistant, whereas approximately 8% of the *O. glaberrima* accessions have the same phenotype of high resistance (Thiémélé et al. 2010). Several major resistance genes such as *RYMV1, RYMV2*, and *RYMV3* have been reported (Albar et al. 2003; Pidon et al. 2017; Thiémélé et al. 2010). *RYMV1* is the most studied and encodes the translation initiation factor eIF(iso)4G1 (Albar et al. 2006). Four *RYMV1* resistance alleles have been identified, named *rymv1-2* through *rymv1-5*, and characterized by single nonsynonymous mutations or short deletions in the central domain of the protein.

Currently, only the *rymv1-2* allele has been introduced in rice varieties (Bouet et al. 2013; Ndjiondjop et al. 2013). Because the deployment of resistance plants has not yet been performed at large scales and over long periods of time, their ability to sustain resistance under field conditions is still unknown. However, under controlled conditions, the resistance-breaking (RB) ability of isolates has been tested after inoculation of 114 and 84 isolates that are representative of the RYMV genetic diversity to Gigante and Tog5681 accessions, respectively (Pinel-Galzi et al. 2007; Traoré et al. 2010). A proportion of the tested isolates was able to overcome the resistance of the *rymv1-2* and *rymv1-3* alleles (9 and 25%, respectively). The molecular mechanism involved in this phenomenon has been described. A direct interaction between the wild-type viral genome-linked protein (VPg) and the eIF(iso)4G1 of susceptible rice species is required for viral infection to occur (Hébrard et al. 2010). Mutations of the *rymv1-2* and *rymv1-3* alleles disrupt this interaction, resulting in the resistance phenotype (Hébrard et al. 2010). However, a residual multiplication of RYMV in resistant plants, as revealed by quantitative reverse-transcription

polymerase chain reaction (RT-PCR) analysis, allows the emergence of mutations in the central domain of the VPg (Poulicard et al. 2010; Traoré et al. 2010). Several convergent nonsynonymous substitutions were found in different strains. The role of the most frequent mutations at positions 41, 48, and 52 was experimentally validated: they restore the protein interaction with resistance alleles (Hébrard et al. 2008, 2010). Stepwise evolutionary processes were observed with the accumulation of RB mutations at positions 41 and 52 against the *rymv1-3* allele or at codon 48 against the *rymv1-2* allele (Pinel-Galzi et al. 2007; Traoré et al. 2010).

In most cases, the adaptability of RYMV isolates is restricted to only one of these two alleles. A glutamic acid/threonine (E/T) polymorphism located at position 49 of the VPg is associated with this contrasted RB ability. Isolates with genotype E49 only break the *rymv1-2*-mediated resistance of Gigante and are referred to as isolates of pathotype E. By contrast, those with the genotype T49 preferentially overcome *rymv1-3*-mediated resistance of Tog5681 and are referred to as isolates of pathotype T (Traoré et al. 2010). A viral fitness assessment showed that T49 is not only a molecular signature of *rymv1-3* RB ability but also a genetic determinant of a

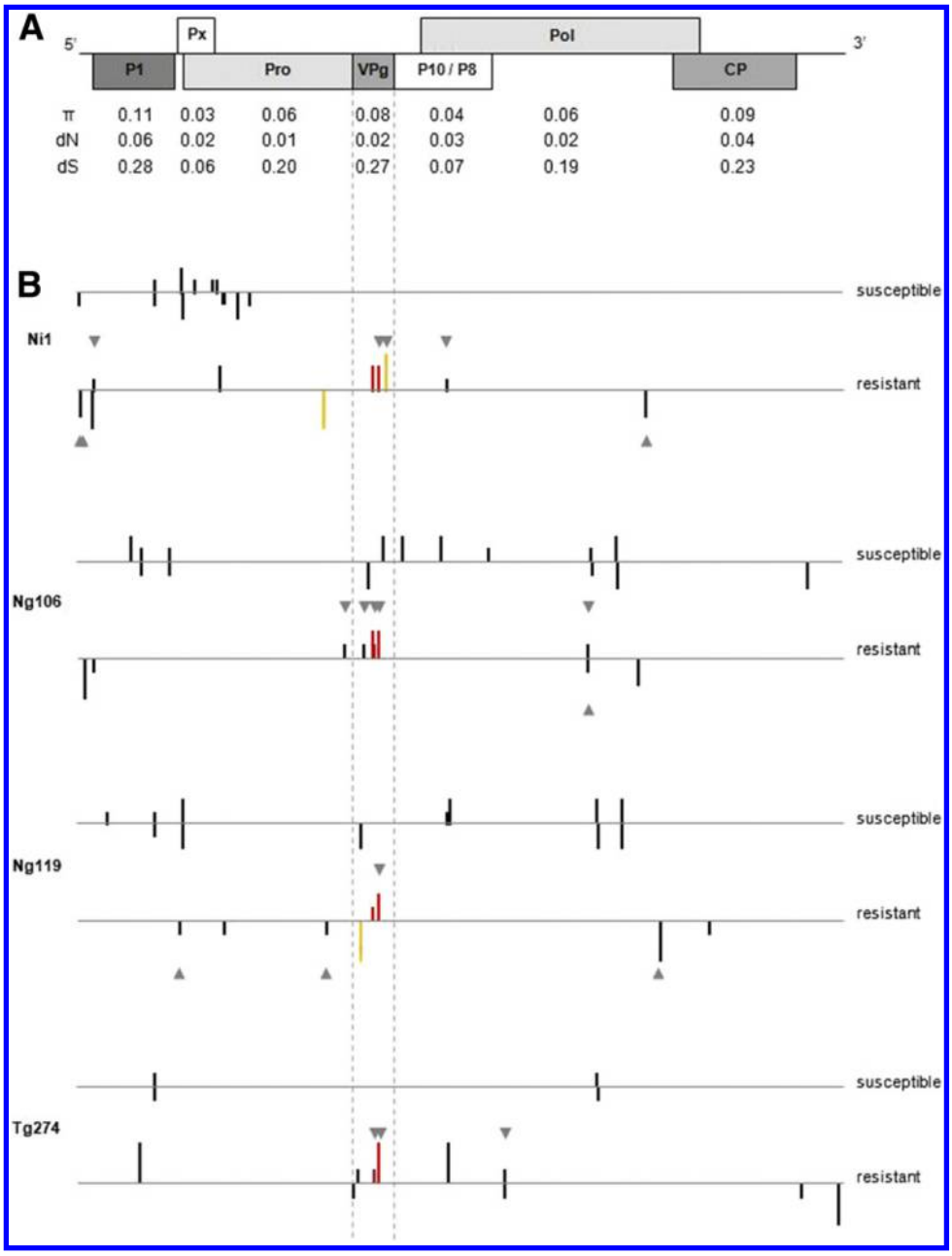

Fig. 1. Genetic diversity of full-length *Rice yellow mottle virus* (RYMV) genomes. **A,** RYMV genomic organization is shown, with boxes and shades of gray representing encoded proteins and increasing levels of genetic diversity (π), respectively. The RYMV genome encodes the movement and silencing suppressor protein (P1), overlapping protein (Px), viral protease (Pro), genome-linked protein (VPg), proteins with unknown functions (P10/P8), viral polymerase (Pol), and capsid protein (CP). The diversity indices (π = total substitution per site, dN = nonsynonymous, and dS = synonymous per site) are reported for each protein based on the 33 published full-length sequences, as previously described (Poulicard et al. 2014). The VPg domain is indicated by dotted lines. **B,** Frequencies and positions of single-nucleotide polymorphisms (SNP) detected by deep sequencing in non-resistance-breaking (RB) isolates (from susceptible plants used as inoculum) and of RB isolates (from *rymv1-5*-resistant plants). Two samples (A and B) for each RB isolate (Ni1, Ng106, Ng119, and Tg274) were analyzed and compiled. Black horizontal and vertical lines indicate the RYMV genome and the SNP, respectively. Nonsynonymous and synonymous mutations are indicated above and below each RYMV genome, respectively. The height of each vertical line represents the SNP frequency class (rare = SNP frequency < 10%, frequent = between 10 to 80%, or fixed = > 80%). Conservation of the mutated sites in all of the full-length available sequences (originated from reference sequences) at a nucleotide and amino acid level is shown by a gray triangle.

past adaptation to *O. glaberrima* in the evolutionary history of RYMV (Poulicard et al. 2012). The East-African strains S4 and S5-S6, located in the center of origin of RYMV, harbor the ancestral trait E49. By contrast, strain S2-S3, which is distributed in West-Africa, harbors the derived trait T49. This region is the geographical distribution area of *O. glaberrima* (Traoré et al. 2005; Trovão et al. 2015). Additionally, the S1 strain is divided into two main lineages, S1wa and S1ca, which correlate to their spatial distribution in West and West-Central Africa, respectively. Several independent T49 fixation events in these two lineages have been inferred phylogenetically, resulting in E/T polymorphism of this strain (Pinel-Galzi et al. 2007). Finally, T49 confers a selective advantage in the susceptible African rice species compared with E49, regardless of the strain (Poulicard et al. 2012). Importantly, four isolates with T49 were efficiently able to overcome both *rymv1-2*- and *rymv1-3*-mediated resistances, suggesting the existence of a new pathotype (Traoré et al. 2006a, 2010). Three of these four isolates belonged to the S1ca lineage. This lineage also revealed a high capacity to overcome *RYMV2*- and *RYMV3*-mediated resistance from Tog7291 and Tog5307 accessions, respectively (Pidon et al. 2017; Pinel-Galzi et al. 2016).

In this study, we assessed the resistance spectrum of the *rymv1-4* through *rymv1-5* alleles against a selection of isolates that are representative of the RYMV genetic and pathogenic diversity, including isolates with T/E49 from the S1ca lineage. This was done to obtain a complete overview of the RB abilities of RYMV toward all of the identified sources of resistance in rice. We identified and characterized a hypervirulent pathotype, named pathotype T′, that is able to overcome all known sources of high resistance. To better understand the adaptive processes of pathotype T′, molecular determinants of resistance breakdown were identified and their functional role was validated. Deep sequencing of the hypervirulent pathotype T′ was performed to investigate the resistance breakdown cases without fixed mutations. The consequences of these findings on the assessment and prediction of the emergence risks of RYMV virulent lineages are discussed in the context of resistance sustainability.

MATERIALS AND METHODS

Plant accessions and viral isolates. Two rice accessions were used as susceptible controls: *O. sativa indica* IR64 and *O. glaberrima* Tog5673 (International Rice Germplasm Collection number 96789). Four *RYMV1*-resistant accessions were assessed: *O. sativa indica* Gigante (*rymv1-2* resistant allele) and *O. glaberrima* Tog5681 (*rymv1-3*), Tog5438 (*rymv1-4*), and Tog5674 (*rymv1-5*) (IRGC 96793, 96751, and 96790, respectively) (Thiémélé et al. 2010). The plants were kept in a growth chamber under 12 h of illumination at 120 µE/m²/s, 28°C, and 60% humidity.

Twenty RYMV isolates were used in this study (Supplementary Table S1). They are representative of the RYMV genetic and pathogenic diversity, and most of these isolates (16 of 20) have previously been inoculated to the *rymv1-2*- and *rymv1-3*-resistant Gigante and Tog5681 accessions (Traoré et al. 2010). In addition to these well-characterized isolates, four new isolates from the S1ca lineage were included in this study as candidates for the new pathotype. They belong to the collection from Niger that was described previously (Traoré et al. 2010) or were recently collected in Togo (Oludare et al. 2016) and have previously been inoculated to the *RYMV2*- and *RYMV3*-resistant Tog7291 and Tog5307 accessions (Pidon et al. 2017; Pinel-Galzi et al. 2016).

Resistance spectrum assessment. The RYMV isolates were inoculated under controlled conditions. Each inoculum was prepared by grinding infected leaves (0.1 g/ml) in a 0.1 M phosphate buffer at pH 7.2. Extracts were mixed with a 600-mesh carborundum and then rubbed on the leaves of 14-day-old rice seedlings. Each RYMV isolate had previously been multiplied in the susceptible rice variety IR64 for further experiments. For the resistance assessment, each isolate was inoculated onto 18 to 24 plantlets of each resistant accession (5 plants by 4 pots) and onto 8 to 10 susceptible control plantlets. Leaves were collected 2 months after inoculation. Symptomatic plants with typical yellow mottling were analyzed individually via double-antibody sandwich enzyme-linked immunosorbent assay (DAS-ELISA) with a polyclonal antiserum raised against an RYMV isolate from Madagascar (Fargette et al. 2002). Asymptomatic plants of the same pot were pooled together and then analyzed individually in the case of a positive pool.

Sanger sequencing and validation of RB mutations. For each viral isolate–plant accession modality, two infected plants were randomly selected. For the new pathotype T′ candidate isolates, five samples per modality were selected. Total RNA was extracted using the RNeasy Plant Mini kit (Qiagen). The VPg and its 5′ and 3′ neighboring regions were specifically amplified via RT-PCR, as previously described (Hébrard et al. 2006), and sequenced using the Sanger technique. To identify RB mutations, the VPg sequences of the RB genotypes obtained via the Sanger technique were aligned using CLUSTALW with default parameters and compared with those of the corresponding wild-type genotype. To validate the functional role in resistance breakdown of the new convergent mutations R38Q and T43A in the VPg, as well as the influence of the T/E49 polymorphism, the mutants Cia38, Cia38/49, Cia43, and CIa43/49 were constructed via directed mutagenesis of the infectious clone CIa (T49) with a QuickChange Site-Directed Mutagenesis Kit (Agilent) (Pinel-Galzi et al. 2007; Traoré et al. 2010). The new clones were fully sequenced by the Sanger technique, as described previously (Fargette et al. 2004), to validate their conformity. Transcription of mutated clones and inoculation of viral RNA in the susceptible rice variety IR64 were performed as previously described (Poulicard et al. 2010). To assess the RB ability, each isolate was inoculated onto 15 to 20 plantlets of each resistant accession and onto 10 susceptible control plantlets. RB analysis was conducted as described above using DAS-ELISA for RYMV detection on symptomatic leaves 2 months after inoculation. The VPg of two samples randomly selected from each mutant was sequenced via the Sanger technique as described above to confirm the presence of the inserted mutations.

Deep sequencing. For each of the isolates Ni1, Ng106, Ng119, and Tg274, two plants named A and B (from the Tog5674 accession, *rymv1-5* allele and the corresponding inoculum from the susceptible control variety IR64) were randomly selected. The RYMV genome was amplified using a two-step process. First, specific full-length reverse transcription was performed using the primer D_{AS} (Fargette et al. 2004) and PrimeScript reverse transcription (Takara Bio Inc.). Second, the RYMV genome was amplified in two overlapping fragments using the primers A_S/B_{AS} and C_S/D_{AS} (Fargette et al. 2004) and ExTaq polymerase (Takara Bio Inc.). Libraries were constructed using 6-bp barcodes to allow for multiplexing, as previously described (Mariac et al. 2014). Briefly, PCR fragments of the same sample were bulked in equal equimolar conditions and sheared to a mean target size of 400 bp. Fragments were then repaired, ligated, nick filled in, and amplified via real-time PCR to complete the adapters and generate libraries that were ready for cluster generation and sequencing. Pair-end sequencing (2 × 150 bp) was performed on an Illumina MiSeq v3 platform at the CIRAD facilities (Montpellier, France), with approximately 12 pmol of the DNA libraries deposited on the flow cell.

Demultiplexing was undertaken using a script that sorts reads as a function of a given list of barcodes (script available at DEMULADAPT; https://github.com/Maillol/demultadapt). The fastq files are available on the National Center for Biotechnology Information Sequence Read Archives (number SRP116739). Reads were analyzed using Galaxy workflows (Afgan et al. 2016; Giardine et al. 2005) implemented on the South Green bioinformatic platform. Briefly, reads were filtered based on their length and mean quality values (Q > 35), and adapters were removed using

Cutadapt (Martin 2011) with the following parameters: minimum overlap length = 7 and minimum length after trimming = 35. Reads of each sample from susceptible plants (inoculum) were first mapped to the closest available full-length virus sequence to obtain a consensus sequence. In a second step, reads of each RB sample were mapped against this consensus sequence. Mapping was performed using BWA-MEM (Li and Durbin 2010) with the following parameters: maximum edit sequence = 0.06 and maximum difference in the seed = 5. After a sorting step with SortSam, the optical duplicates were removed with MarkDuplicates from Picard tools (http://picard.sourceforge.net), and reads were then realigned using Realigner Target Creator and Indel Realigner from the GATK package (McKenna et al. 2010). Single-nucleotide polymorphisms (SNP) were called using Samtools (Generate pileup) (Li et al. 2009) and Varscan Pileup2snp (Koboldt et al. 2009) with the following parameters: minimum base quality = 30, minimum read depth = 100, minimum supporting reads to call a variant = 10, and minimum variant allele frequency = 0.03. For the RB samples, only the SNP that were not detected in the inoculum (from susceptible plants) or SNP for which there was a frequency increase compared with the inoculum were considered. The ORF and the SNP positions were numbered after a realignment step with the reference sequence of the infectious clone CIa. Site conservation was determined according to the 33 published full-length sequences (Rakotomalala et al. 2013). SNP were considered to be rare or fixed when their frequency was < 10% or > 80%, respectively. VPg haplotypes were analyzed using a three-step Galaxy process (Bedtools, Samtools BAM-to-SAM, and SAM-to-Fasta). Then, the alignment was manually curated to remove incomplete reads, and the haplotype frequencies were calculated with DNAsp (Rozas et al. 2003).

RESULTS

RYMV RB ability against highly resistant accessions. Twenty RYMV isolates were inoculated under controlled conditions onto four resistant plant accessions of the *RYMV1* allelic series (Fig. 2). The viral isolates were selected to be representative of the RYMV genetic and pathogenic diversity based on the previous results of their phylogeny and their RB ability in the Gigante and Tog5681 accessions (Pinel-Galzi et al. 2007; Traoré et al. 2010). Isolate candidates for the new pathotype able to overcome both *rymv1-2* and *rymv1-3* alleles were included in this study in order to provide a deeper assessment of their virulence spectrum. Viral adaptability was evaluated as a qualitative parameter defined by the ability of a given isolate to overcome the resistance of a given accession. By contrast, the resistance spectrum conferred by a given

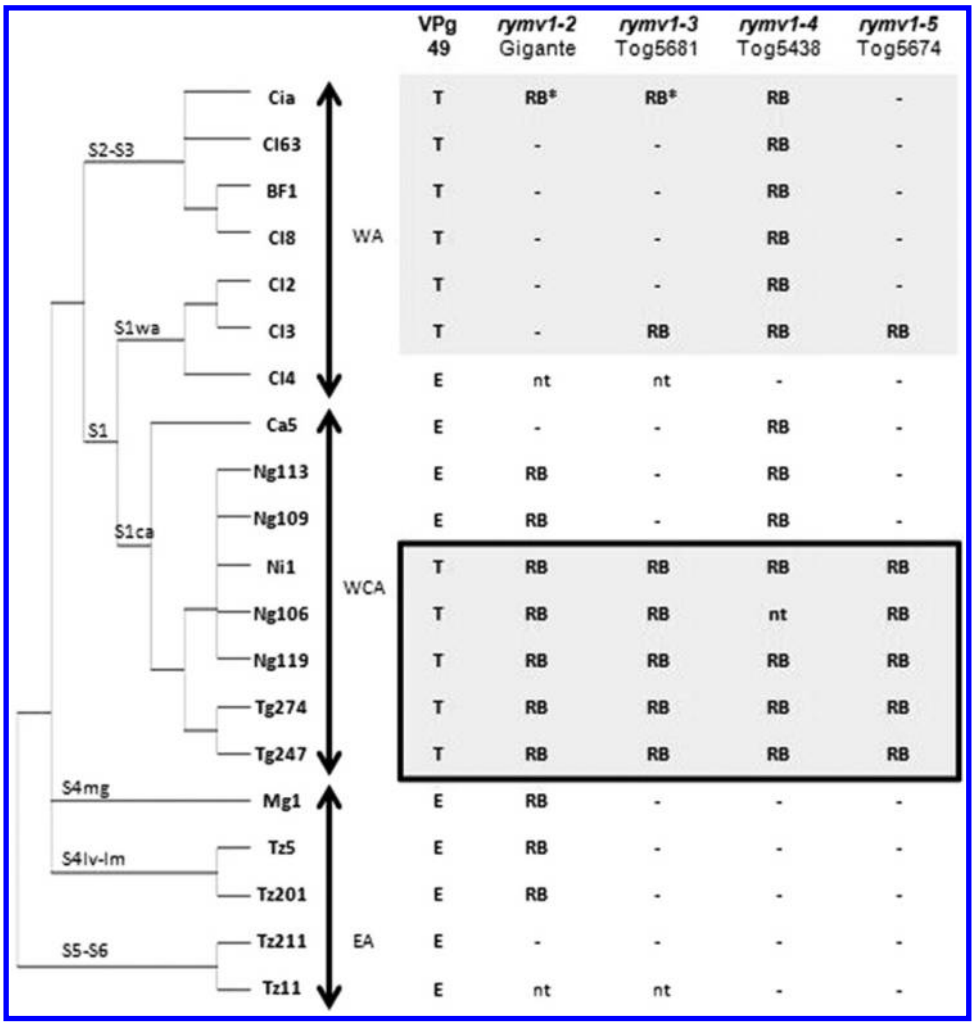

Fig. 2. Resistance-breaking abilities of *Rice yellow mottle virus* (RYMV) isolates. One accession (Gigante, Tog5681, Tog5438, and Tog5674) with each *RYMV1*-resistant allele (*rymv1-2, rymv1-3, rymv1-4*, and *rymv1-5*) was challenged against 20 isolates from different strains (S1 to S6) that originated from West Africa (WA), West-Central Africa (WCA), and East Africa (EA). Taxonomic positions of the isolates are inferred from the cladogram reconstructed by parsimony from their coat protein sequence. The viral adaptability depends on the amino acid at position 49 of the viral genome-linked protein (VPg) (threonine = T or glutamic acid = E) and on the *RYMV1* allele. Isolates of the pathotypes T and T′ are shaded in gray. The new pathotype T′ able to overcome all the *RYMV1* alleles is indicated by a black box. RB = ability of resistance breakdown, – = no resistance breakdown, * = previously published (Pinel-Galzi et al. 2007, 2016; Pidon et al. 2017; Traoré et al. 2010), and nt = not tested.

resistance allele was evaluated as a quantitative parameter that was estimated from the 20 RYMV isolates representative of the viral diversity in Africa.

As expected, susceptible controls (8 to 10 inoculated plants/isolate) were all infected (data not shown). Most of the resistant plants (18 to 24 inoculated plants/accession/isolate) did not develop any symptoms and viral multiplication was not detected by DAS-ELISA (Fig. 2; Supplementary Table S2). However, typical RYMV symptoms were observed for 520 of the 1,605 inoculated plants (i.e., 32% of the total number of resistant plants) 1 to 2 months after inoculation. Resistance breakdown was confirmed by DAS-ELISA, and RYMV was detected in each symptomatic plant. The resistant rice accessions and the RYMV isolates showed variable resistance spectra and different RB abilities (Fig. 2). Of the 80 viral isolate–plant accession modalities, 35 led to symptoms within 70% of the inoculated plants. As previously described (Pinel-Galzi et al. 2007; Traoré et al. 2010), the resistance of the Gigante accession (*rymv1-2* allele) was overcome by several isolates of pathotype E and the resistance of the Tog5681 accession (*rymv1-3* allele) by isolates of pathotype T (Table 1). Additionally, and as expected, the five isolates with T49 originating from West-Central Africa were able to overcome the resistance provided by both the *rymv1-2* and *rymv1-3* alleles. Consistently, the adaptability of the Ng106 and Ng119 isolates to the Tog5681 accession was previously reported (Traoré et al. 2010).

For the first time, the resistance spectra of the *O. glaberrima* accessions Tog5438 and Tog5674, which harbor the *rymv1-4* and *rymv1-5* alleles, respectively, were assessed with the same isolates. Similarly to the Tog5681 accession, the two tested accessions showed an efficient resistance to isolates from East Africa (Fig. 2). A different trend was observed with West and West-Central African isolates. On the one hand, *rymv1-4*-mediated resistance from the Tog5438 accession was overcome by most isolates from the S1 and S2-S3 strains, regardless of the pathotype. On the other hand, *rymv1-5*-mediated resistance showed a spectrum similar to that mediated by the *rymv1-3* allele. Interestingly, the isolates from West-Central Africa (S1ca lineage) with a threonine at position 49 of the VPg and that were able to overcome the resistance of the Tog5681 accession also broke the resistance of the Tog5674 accession. Hence, these results confirmed that the isolates with T49 from the S1ca lineage defined a new pathotype, referred to hereafter as pathotype T′. Pathotype T′ is characterized by hypervirulence (i.e., the ability to overcome resistance mediated by all of the *RYMV* resistance genes and alleles).

RB mutations detected via VPg sequencing and validated by directed mutagenesis. To better understand the adaptive processes of pathotype T′, 80 infected samples were randomly selected, and their VPg gene was amplified and sequenced via the Sanger technique. Only nucleotide transitions (purine to purine or pyrimidine to pyrimidine) were detected. They all resulted in nonsynonymous substitutions of amino acids with biochemical properties that were different from those of the wild-type isolates. The substitutions were located at positions 41, 43, and 52 of the VPg gene (Table 2). Consistent with previous findings (Pinel-Galzi et al. 2007; Traoré et al. 2010), we found a histidine-to-tyrosine substitution at position 52 (H52Y) in the *rymv1-2* and *rymv1-3* RB genotypes and a serine-to-proline substitution at position 41 (S41P) in the *rymv1-3* RB genotypes. For the first time, the VPg sequences of the *rymv1-4* and *rymv1-5* RB genotypes were sequenced. In the *rymv1-4* RB genotypes, substitutions of threonine to alanine at position 43 (T43A) and S41P were observed. The substitution T43A was described previously in the *rymv1-2* RB genotypes (Pinel-Galzi et al. 2007). In the *rymv1-5* RB genotypes, the substitutions were restricted to S41P and H52Y. Importantly, a mix between the wild-type nucleotide and its mutated alternative was found in 15 samples (Table 2; Supplementary Table S3), which indicates intrahost diversity and evolution of the viral population during the RB processes. Additionally, in three RB samples, two emerging mutations, S41P and either T43A or H52Y, were detected in the same sample; however, this sequencing technique cannot determine whether the samples contained a double-mutated genotype or two single mutants (Table 2). Two synonymous substitutions at positions 48 and 62 were detected in two *rymv1-4* RB genotypes; they were isolate specific and belong to the Ng119 isolate. Thirty samples from the other strains and lineages were sequenced. The same major substitutions, S41P and H52Y, were identified. In addition to the T43A substitution, an asparagine-to-tyrosine substitution at position 42 (N42Y) was detected in the *rymv1-2* RB genotypes from East Africa. An arginine-to-glutamine substitution at position 38 (R38Q) was identified in the *rymv1-4* RB genotype from West Africa. A new specific substitution of the Ng109 isolate (i.e., a glutamic acid-to-lysine substitution at position 29 [E29K]) was detected in three *rymv1-4* RB genotypes. Altogether, the most frequent mutations in the current study, as well as in previous studies (Pinel-Galzi et al. 2007; Traoré et al. 2010), revealed convergence in the RB molecular determinants in the *RYMV1* allelic series.

Contrary to the role of the mutations at positions 41, 48, and 52, the role of the VPg convergent mutations R38Q and T43A in resistance breakdown have not been previously validated. We performed directed mutagenesis to introduce these mutations in the infectious RYMV clone and inoculated the mutants into plants from the *RYMV1* allelic series (except *rymv1-4*, because of its low range and efficiency for resistance against isolates from West and West-Central Africa). The RB ability of each mutated clone was tested in combination with the E/T residue at position 49. The infectious clone CIa was used as a negative control in our study. Notably, this genotype has been previously reported to often overcome the resistance of *rymv1-3* (and rarely *rymv1-2*) via the emergence of de novo RB mutations. The CIa52 genotype was used as a positive control. As expected, this genotype was efficient against *rymv1-5* resistance, as well as against *rymv1-2* and *rymv1-3* resistance (Table 3). However, the RB efficiency of the CIa52/49 genotype was restricted to *rymv1-2*-mediated resistance. Replacing T49 with E49 prevented the efficiency of the H52Y mutation to overcome *rymv1-3*- and *rymv1-5*-mediated resistances.

The mutation T43A has already been reported in *rymv1-2* and *rymv1-3* RB mutants. In this study, it was detected to be associated with resistance breakdown in the three accessions tested (Gigante, Tog5681, and Tog5674) (>80% infected plants). The CIa43 genotype showed the same RB ability and efficiency as the CIa52 genotype. The combination of the T43A and T49E mutations prevented the infection of all *RYMV1*-resistant accessions, including Gigante. The mutation R38Q, which has already been reported in *rymv1-2* RB mutants, was not able to overcome the *rymv1-2* resistance in our study, even when combined with T49E. Interestingly, although it was never detected experimentally, the R38Q mutation inserted alone in the infectious clone CIa allowed it to overcome *rymv1-3*- and *rymv1-5*-mediated resistances (>60% of infected plants). In combination with T49E, the R38Q mutation lost its RB function against resistant *O. glaberrima* accessions. Altogether, we conclude that single nonsynonymous mutations inserted in the central domain of the VPg at a restricted number of conserved positions allowed the breakdown of resistance in accessions with the *RYMV1* allelic series depending on the residue at position 49 (Fig. 3).

TABLE 1. Number and percentage of *Rice yellow mottle virus* (RYMV) isolates from pathotypes E, T, and T′ that are able to infect rice accessions with *RYMV1* resistance alleles

Accessions	E	T	T′	Total
rymv1-2/Gigante	6/9 (67%)	1/6 (17%)	5/5 (100%)	12/20 (60%)
rymv1-3/Tog5681	0/9 (0%)	2/6 (33%)	5/5 (100%)	7/20 (35%)
rymv1-4/Tog5438	3/9 (33%)	6/6 (100%)	4/4 (100%)	13/19 (68%)
rymv1-5/Tog5674	0/9 (0%)	1/6 (17%)	5/5 (100%)	6/20 (30%)

However, 66% of the sequenced VPg from the RB samples showed no mutations in comparison with the sequence from the wild-type isolate (54 of 80 samples from the hypervirulent pathotype T′ and 18/30 samples from the other pathotypes) (Table 2). Several hypotheses could explain this phenomenon: (i) isolates possess some intrinsic genetic properties to overcome resistant alleles without mutation, (ii) VPg mutations with a low frequency are not detected via Sanger sequencing, or (iii) RB mutations occur outside the VPg gene in the RYMV genome.

RB mutations detected in the hypervirulent pathotype T′ via deep sequencing. To test these hypotheses, we performed deep sequencing of the full-length RYMV genome on samples with or without emerging or fixed mutations detected via Sanger sequencing. We focused on the Tog5674 accession (*rymv1-5*) and on the hypervirulent pathotype T′ (isolates Ni1, Ng106, Ng119, and Tg274 of the S1-ca strain), which showed the widest resistance and RB spectra, respectively. For each isolate, two independent RB samples (namely, A and B) were compared with the inoculum originated from susceptible plants (Fig. 1B). After amplification of the full-length RYMV genome in two overlapping fragments and the preparation of the libraries, tagged samples were multiplexed and sequenced using MiSeq Illumina technology.

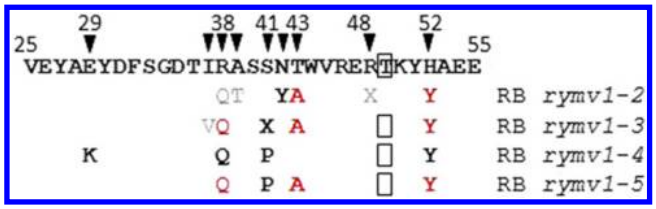

Fig. 3. Location of the *Rice yellow mottle virus 1* (*RYMV1*) resistance-breaking (RB) substitutions in the viral genome-linked protein (VPg). Single non-synonymous RB mutations restricted to the central domain of the VPg at conserved positions allow the resistance breakdown of Gigante (*rymv1-2*), Tog5681 (*rymv1-3*), Tog5438 (*rymv1-4*), and Tog5674 (*rymv1-5*), depending on the residue at position 49 (boxed). Dark (red) and bold letters = RB mutations found by sequencing and validated in this study, gray letters = potential RB mutations confirmed by mutagenesis, black and bold letters = found by sequencing in this study, and light gray letters = previously reported. X at position 41 = proline (P)/alanine (A) and X at position 48 = glutamic acid (E)/glycine (G)/isoleucine (I)/valine (V). K = lysine, Q = glutamine, T = threonine, and Y = tyrosine.

In total, 42 polymorphic sites were found along the RYMV genome from the inocula (susceptible plants) (Fig. 1B). Among them, 24 sites have been previously identified comparing the 33 published sequences representative of the RYMV genetic diversity. The number and positions of the polymorphic sites along the genome were highly variable, depending on the isolates. In total, 25 polymorphic sites were common in susceptible and resistant plants, and they were considered in the rest of the study only if their frequency increased compared with the inoculum. In the resistant plants, 42 RB candidate sites were found along the RYMV genome (Fig. 1B; Supplementary Table S4). They were located discontinuously in three main diversity hotspots in the 5′ noncoding region, the VPg, and the polymerase genes. In total, 62% of the mutated sites were found to be strictly conserved at the nucleotide level compared with 33 RYMV sequences representative of RYMV genetic diversity (Fig. 1B). Only 25% of the mutations were fixed or close to being fixed (SNP frequency in the viral populations > 80%), whereas 52% of the mutations were rare (SNP frequency < 10%) and could not be detected via Sanger sequencing (Supplementary Table S5). Considering only the coding domains, 32 mutated sites were identified, and 23 of these (i.e., 72%) resulted in nonsynonymous substitutions. Interestingly, only 11 of these 23 mutated sites were strictly conserved at the amino acid level across the diversity of RYMV. They are the best candidates to explain the RB cases because the reference isolates exclusively originated from susceptible rice varieties. Nonsynonymous mutations represented 8% of the VPg amino-acids and 75% of the total number of mutations (6 of 8 mutations) in the VPg (Supplementary Table S6). Four of eight sites (positions 23, 41, 43, and 52) were strictly conserved in the reference sequences and were variable in our RB samples.

Interestingly, very few mutations emerged independently in different modalities. We found only three cases of identical mutations between two samples of the same isolate inoculated with Ni1 and Ng119 in the protease and the VPg (Fig. 1B). These mutations were all fixed in the resistant plants, and one of these mutations in the VPg was also detected at a frequency of 49% in the inoculum originating from susceptible plants. In addition, three convergent mutations were found in two to six samples (from two to four different isolates) (Fig. 1B). All of these mutations were nonsynonymous substitutions located in the VPg at strictly conserved positions in the reference sequences (originating from

TABLE 2. *Rice yellow mottle virus* gene *RYMV1* resistance-breaking mutations in the viral genome-linked protein (VPg) of the isolates from the hypervirulent pathotype T′[a]

Isolates	*rymv1-2* Gigante	*rymv1-3* Tog5681	*rymv1-4* Tog5438	*rymv1-5* Tog5674
Ni1	RB	RB	S41P^{m}+T43A^{m}, RB	S41P, S41P^{m}, H52Y^{m}, RB
Ng106	RB	RB	nt	S41P^{m}+H52Y^{m}, H52Y, RB
Ng119	H52Y, RB	S41P, RB	syn^{m}, RB	H52Y, RB
Tg274	H52Y	S41P, H52Y^{m}, RB	RB	H52Y, H52Y^{m}, RB
Tg247	H52Y	H52Y, RB	RB	S41P^{m}+H52Y^{m}, H52Y, RB

[a] RB = resistance breakdown with no mutation detected, superscript "m" = mix of mutated and wild-type VPg residues in the same sample (i.e., an emerging mutation), + indicates different mutations found in the same sample, and nt = not tested.

TABLE 3. Validation of resistance-breaking (RB) mutations in the viral genome-linked protein (VPg) gene of the infectious clone CIa, depending on the T/E residue at position 49[a]

	CIa	CIa49	CIa52	CIa52/49	CIa43	CIa43/49	CIa38	CIa38/49
	T	E	T	E	T	E	T	E
Susceptible	+	+	+	+	+	+	+	+
rymv1-2	–[b]	–[c]	+	+	+	–	–	–
rymv1-3	–[b]	–	+	–	+	–	+	–
rymv1-5	–	–	+	–	+	–	+	–

[a] Symbols: + = RB and presence of the inserted substitutions and – = no infection.
[b] No infection in this study but RB with additional mutation acquisition previously published (Poulicard et al. 2014; Traoré et al. 2010).
[c] RB obtained in this study but with additional mutation acquisition.

susceptible plants) (Fig. 1A). These convergent mutations, detected via deep sequencing, correspond to mutations that were previously found in other samples via Sanger sequencing. The mutations H52Y, S41P, and T43A were found in six, five, and three samples, respectively, of eight samples total. Their frequency was highly variable depending on the sample (27 to 97, 5 to 32, and 6 to 10%, respectively). These substitutions were not detected in the inoculum. Haplotype analysis of the central domain of the VPg revealed that, in most of the samples, the mutations at positions 41, 43, and 52 were present independently in different RB genotypes (i.e., no mutation accumulation was detected) (Table 4). The unique exception was sample B of the isolate Ng119, in which all of the reads with the S41P mutation (6%) also contained the H52Y mutation.

Overall, our study showed that, for the eight samples analyzed from the hypervirulent pathotype T′, (i) RB genotypes always contained mutations, (ii) most of the mutations were not fixed and could not be detected via Sanger sequencing, and (iii) RB mutations also occurred in genes other than VPg gene. However, considering the mutations identified via the Sanger and Illumina methods, the mutations in the VPg could explain all of the cases of resistance breakdown, except for that in Ng106 B, even with mutation frequencies below 32% (for instance, in Ng106 A) (Table 4).

DISCUSSION

Strategies for breeding rice to resist RYMV have to consider several variable constraints such as the resistance spectra of the plants and RB abilities of the virus. Working under controlled conditions, our aim was to better assess and understand the influence of these parameters to predict resistance sustainability and to optimize deployment strategies, minimizing viral adaptation. Resistance breakdown first requires the emergence of mutations at the intrahost level. Although we cannot exclude the involvement of different RYMV genes in *RYMV1*-associated RB mechanisms as previously reported (Poulicard et al. 2014), VPg has a predominant role, as expected from the direct interaction with the eIF(iso)4G1 resistance factor. In our study, we showed that single mutations in the central part of the VPg are enough to overcome the entire *RYMV1* allelic series. We confirmed that RB mutations occurred only at a restricted number of sites in this highly conserved protein and that the various RYMV strains and lineages followed strong convergent mutational pathways. In addition to the substitution H52Y, new multifunctional RB mutations were revealed at positions 38 and 43. The structural features of the VPg, an intrinsically disordered protein (Hébrard et al. 2010). and the vicinity of mutations in the same VPg–MIF4G interaction domain explained this multifunctionality. Mutation convergence occurred not only in different isolates but also in different resistant hosts, and the efficiency range of the H52Y, R38Q, and T43A mutations covered all of the *RYMV1* alleles. The emergence of these mutations on one resistant accession could lead to the resistance breakdown of the others and could invalidate deployment strategies that alternate resistance alleles. In contrast to the previous hypotheses, we revealed, using deep sequencing, that mutation accumulation did not always occur, and that RB mutations emerged independently in different haplotypes. Unfortunately, when single mutations are sufficient to overcome resistance genes, the resistance sustainability is predicted to be low (Fabre et al. 2009; Harrison 2002; Lecoq et al. 2004). Additionally, the role of the viral population in the RB mechanism was discovered with, for the first time, nonfixed mutations that were able to explain the RB phenotype. The fact that this phenomenon is not restricted only to the hypervirulent pathotype T′ suggests intrapopulation complementation (i.e., a minor mutated genotype helps to maintain the wild-type genotype in the viral population) (Andino and Domingo 2015). Moreover, preliminary experiments suggest that the mutated clones CIa38and CIa43 are not associated with fitness losses in susceptible plants (*O. sativa,* variety IR64, and *O. glaberrima*, accession Tog5673). Resistance sustainability is predicted to decrease when the fitness penalty induced by RB mutations is low in susceptible hosts (Fabre et al. 2009; Harrison 2002; Lecoq et al. 2004).

Our data allowed for a complete assessment of the *RYMV1* allelic series, generating an overview of the RB prediction efficiency when facing RYMV diversity. The alleles *rymv1-3* (Tog5681) and *rymv1-5* (Tog5674) exhibited the widest resistance range. This result was expected, particularly when taking into account the nature of the resistance mutations; namely, a deletion of three residues (ΔRDD 322 to 324) and a combination of a lysine-to-asparagine substitution (K312N) and another short deletion (ΔLTG 313 to 315). Structurally close, the resistance sustainability of these two alleles was similar. Nevertheless, the relative complexity of *rymv1-5* may result in more sustainability. Indeed, experiments in double yeast-hybrid assays suggest a lower residual interaction of the wild-type VPg with the mutated central domain of eIF(iso)4G1, mimicking the *rymv1-5* allele (Supplementary Fig. S1). In comparison, the

TABLE 4. Comparison of classical (Sanger) and deep-sequencing (Illumina) data for the viral genome-linked protein (VPg) of isolates from the hypervirulent pathotype T′

Isolates	Samples	Sanger[a]	Illumina (total)[b]
Ni1	A	RB	41 (8%) or 43 (10%)
	B	52^{m}	41 (14%) or 52 (28%)
Ng106	A	41^{m}+52^{m}	41 (32%) or 43 (10%) or 52 (29%)
	B	RB	RB
Ng119	A	52	41 (5%) or 52 (83%)
	B	52	**41+52** (6%) or 52 (73%)
Tg274	A	52	52 (97%)
	B	52^{m}	43 (6%) or 52 (48%)

[a] RB = resistance-breaking event but no mutation detected, + = combination of several mutations in the same sample (classical sequencing data), and superscript "m" = mix of mutated and wild-type VPg residue in the same sample. Haplotypes combining two mutations are indicated in bold (deep sequencing data).

[b] Numbers refer to the mutation position in the VPg, and the percentage in parenthesis corresponds to the single-nucleotide polymorphism frequency detected via deep sequencing.

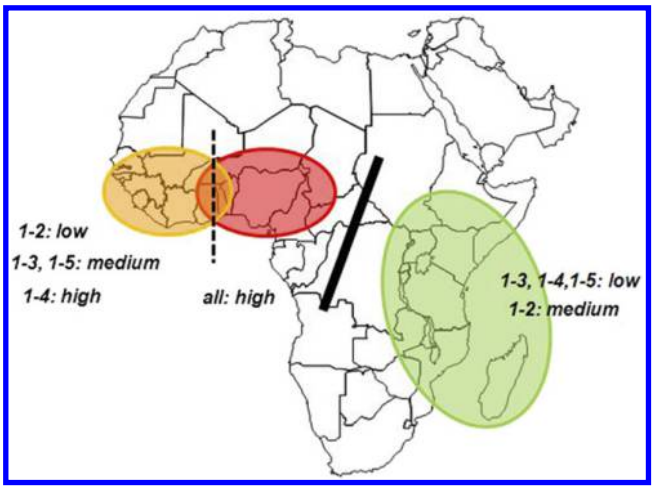

Fig. 4. *Rice yellow mottle virus 1* (*RYMV1*) resistance breakdown risk map: a tool to optimize the *RYMV1* deployment strategy. Defined as low (right), medium (left), or high (center), the resistance breakdown risk assessed here (Table 1) and previously (Pidon et al. 2017; Pinel-Galzi et al. 2007, 2016; Traoré et al. 2010) is shown for the *RYMV1* allelic series according to the geographical distribution of the strains (Pinel-Galzi et al. 2015; Traoré et al. 2005). The resistance breakdown risk is defined based on the representative isolates' ability to overcome the resistance of the corresponding alleles. Weak (dotted line) and strong (plain line) barriers to virus propagation are illustrated based on dispersal rate and rice landscape (dense or sparse cultivation; see Discussion).

rymv1-4 (Tog5438) and *rymv1-2* (Gigante) alleles are characterized by the same single substitution, a change from glutamic acid to lysine in very similar molecular environments (at positions 309 and 321, respectively); however, they show very different resistance spectra. The allele *rymv1-4* in Tog5438 was the least sustainable of the tested *O. glaberrima* alleles, and is only efficient toward the East-African isolates (strains S4 to S6 with E49), whereas the allele *rymv1-2* in Gigante (*O. sativa*) is efficient against the strain S2/S3 (with T49) from West Africa (Fig. 2). These differences can be explained by the crucial role of T49, identified as a preadaptation of RYMV to the African rice host, in the ability to overcome the resistance alleles of *RYMV1* originating from *O. glaberrima*. Thus, after gathering the pathogenic data obtained from this study and previous studies (Pinel-Galzi et al. 2007; Traoré et al. 2010), as well as the spatial distribution of the RYMV strains and lineages in Africa (Fargette et al. 2004; Pinel-Galzi et al. 2009; Pinel-Galzi et al. 2015; Traoré et al. 2006a; Trovão et al. 2015), a risk map of *RYMV1* resistance breakdown was proposed (Fig. 4). In East Africa, the RB risk appeared to be low globally, with isolates from strains S4 and S5-S6 unable to overcome the *RYMV1* resistance from *O. glaberrima* accessions. In West-Central Africa, the risk level appeared to be very high, with the isolates from the hypervirulent pathotype T′ (lineage S1-ca with T49) able to overcome all of the *RYMV1* resistance alleles. Additionally, the isolates from the S1-ac lineage with E49, also distributed in this area, showed an RB ability against Gigante and Tog5438. Finally, the situation in West Africa appeared to be intermediate, with a medium risk on the resistance sources, particularly for Tog5681 and Tog5674.Our risk map was generated based on the results obtained from available resistant accessions, mostly of African rice accessions. However, the *O. glaberrima* accessions are not usable at a large scale because of their low yield. Their resistance spectra and efficiency should be compared with those of the corresponding near-isogenic lines. Indeed, a host's genetic background can modulate the frequency of resistance breakdown, as has been shown for the *pvr2* locus (another translation initiation factor involved in resistance to viruses) (Quenouille et al. 2016). Altogether, our results suggested that the introgression of high resistance genes and alleles into high-yielding *O. sativa* varieties could be beneficial in the East African region, with a global low risk of resistance breakdown. Concerning West Africa, we found that the isolates from the strain S2-S3 showed a low *rymv1-3* RB ability, contrary to previously published data. Because the *rymv1-3* (Tog5681) and *rymv1-5* (Tog5674) resistance alleles showed similar resistance spectra, we cannot exclude the possibility that the efficiency of the strain S2-S3 in breaking *rymv1-5*-mediated resistance has been underestimated. The factors involved in this response variability such as viral isolate selection or experimental conditions have not yet been identified and should be investigated more deeply. In our study, we assessed the first step of the viral adaptation to resistant accessions (i.e., the qualitative ability to overcome resistance). Different isolates that are able to overcome Tog7291 (*RYMV2*) show high or very low frequencies of RB events (Pinel-Galzi et al. 2016). In future studies, measures of variability and frequency should be performed to quantify and predict the RB risks in real conditions.

In West-Central Africa, we identified that the hypervirulent pathotype T′ is able to overcome all of the resistance alleles of *RYMV1*, even the most efficient ones, *rymv1-3* and *rymv1-5*. Isolates of this pathotype are able to infect sources of resistance carrying the *RYMV2* and *RYMV3* resistance alleles (Pidon et al. 2017; Pinel-Galzi et al. 2016). Preliminary results also suggested resistance breakdown of the Tog5672 accession (carrying both *rymv1-4* and *RYMV2*). The molecular signatures involved in the intrinsic properties of this new pathotype are under investigation. Analyses of the full-length sequences identified an arginine-to-lysine mutation at position 22 of the VPg as a candidate. The impact of this polymorphism and its combination with T49 on the RB ability of RYMV has to be tested. The hypervirulent pathotype is more abundant than previously suspected. It has been detected in the neighboring countries Nigeria, Niger, and Togo, and its geographical distribution should be monitored, especially in Benin, Burkina-Faso, Cameroon, and Chad. The dispersal risk of RB genotypes can only be realistically estimated if taking into account the overall dispersal rate of the virus, the corridors of propagation, and the agroecological barriers to transmission, information made recently available for RYMV (Pinel-Galzi et al. 2015; Trovão et al. 2015). A spatiotemporal model for RYMV diffusion has been proposed, with an overall dispersal rate of approximately 15 km/year (Trovão et al. 2015). Strain circulation between West and West-Central Africa was hindered for a long time by the scarcity of rice cultivation in the "yam belt" separating the two regions (Pinel-Galzi et al. 2015). This barrier is now fading with the current intensification of rice cultivation, especially along the Niger and Benue rivers, which is now an efficient corridor of propagation of the virus across the two regions (Trovão et al. 2015). By contrast, the large forests of the Democratic Republic of the Congo, with sparse rice cultivation, still constitute an efficient barrier to the spread of RYMV between West-Central and East Africa (Pinel-Galzi et al. 2015; Trovão et al. 2015). Hence, in East Africa, the sustainability of future lines introgressed with *RYMV1* alleles from *O. glaberrima* is unlikely to be threatened by preadapted strains of pathotypes T or T′ originating in West Africa (strains S1 to S3) or by strains circulating in East Africa, which all belong to pathotype E (strains S4 to S6) (Fig. 2). By contrast, resistance management in West and West-Central Africa is complex, with possible circulation of the RB genotypes. The data obtained here contribute to the anticipation and possible mitigation of the RB risks in West and East Africa. The deployment strategies of resistant lines will be optimized in an attempt to sustain rice resistance by taking into account the adaptability of RYMV strains, their spatial distribution, and their dispersal rate.

ACKNOWLEDGMENTS

We thank two anonymous reviewers for constructive criticisms of the manuscript.

LITERATURE CITED

Afgan, E., Baker, D., van den Beek, M., Blankenberg, D., Bouvier, D., Čech, M., Chilton, J., Clements, D., Coraor, N., Eberhard, C., Grüning, B., Guerler, A., Hillman-Jackson, J., Von Kuster, G., Rasche, E., Nicola, S., Turaga, N., Taylor, J., Nekrutenko, A., and Goecks, J. 2016. The Galaxy platform for accessible, reproducible and collaborative biomedical analyses. Nucleic Acids Res. 44:3-10.

Albar, L., Bangratz-Reyser, M., Hébrard, E., Ndjiondjop, M., Jones, M., and Ghesquiere, A. 2006. Mutations in the eIF(iso)4G translation initiation factor confer high resistance of rice to *Rice yellow mottle virus*. Plant J. 47:417-426.

Albar, L., Ndjiondjop, M. N., Esshak, Z., Berger, A., Pinel, A., Jones, M., Fargette, D., and Ghesquière, A. 2003. Fine genetic mapping of a gene required for *Rice yellow mottle virus* cell-to-cell movement. Theor. Appl. Genet. 107:371-378.

Allarangaye, M. D., Traoré, O., Traoré, E. V. S., Millogo, R. J., and Konaté, G. 2006. Evidence of non-transmission of *Rice yellow mottle virus* through seeds of wild host species. J. Plant Pathol. 88:307-313.

Andino, R., and Domingo, E. 2015. Viral quasispecies. Virology 479-480: 46-51.

Bakker, W. 1974. Characterisation and ecological aspects of rice yellow mottle virus in Kenya. Ph.D. thesis, Agricultural University, Wageningen, The Netherlands.

Bouet, A., Amancho, A. N., Kouassi, N., and Anguete, K. 2013. Comportement de nouvelles lignées isogéniques de riz irrigué dotées du gène de résistance (*rymv1*) au RYMV en Afrique de l'ouest: Situation en Côte d'Ivoire. Int. J. Biol. Chem. Sci. 7:1221.

Fabre, F., Bruchou, C., Palloix, A., and Moury, B. 2009. Key determinants of resistance durability to plant viruses: Insights from a model linking within- and between-host dynamics. Virus Res. 141:140-149.

Fargette, D., Konate, G., Fauquet, C., Muller, E., Peterschmitt, M., and Thresh, J. M. 2006. Molecular Ecology and Emergence of Tropical Plant Viruses. Annu. Rev. Phytopathol. 44:235-260.

Fargette, D., Pinel, A., Abubakar, Z., Traoré, O., Brugidou, C., Fatogoma, S., Hébrard, E., Choisy, M., Séré, Y., Fauquet, C., and Konaté, G. 2004.

Inferring the evolutionary history of *Rice yellow mottle virus* from genomic, phylogenetic, and phylogeographic studies. J. Virol. 78:3252-3261.
Fargette, D., Pinel, A., Halimi, H., Brugidou, C., Fauquet, C., and Van Regenmortel, M. 2002. Comparison of molecular and immunological typing of isolates of *Rice yellow mottle virus*. Arch. Virol. 147:583-596.
Giardine, B., Riemer, C., Hardison, R.C., Burhans, R., Elnitski, L., Shah, P., Zhang, Y., Blankenberg, D., Albert, I., Taylor, J., Miller, W., Kent, W. J., and Nekrutenko, A. 2005. Galaxy: A platform for interactive large-scale genome analysis. Genome Res. 15:1451-1455.
Harrison, B. D. 2002. Virus variation in relation to resistance-breaking in plants. Euphytica 124:181-192.
Hébrard, E., Pinel-Galzi, A., Bersoult, A., Siré, C., and Fargette, D. 2006. Emergence of a resistance-breaking isolate of *Rice yellow mottle virus* during serial inoculations is due to a single substitution in the genome-linked viral protein VPg. J. Gen. Virol. 87:1369-1373.
Hébrard, E., Pinel-Galzi, A., and Fargette, D. 2008. Virulence domain of the RYMV Genome-Linked Viral Protein VPg towards rice *rymv1-2*-mediated resistance. Arch. Virol. 153:1161-1164.
Hébrard, E., Poulicard, N., Gérard, C., Traoré, O., Wu, H. C., Albar, L., Fargette, D., Bessin, Y., and Vignols, F. 2010. Direct interaction between the *Rice yellow mottle virus* VPg and the central domain of the rice eIF(iso)4G1 factor correlates with rice susceptibility and RYMV virulence. Mol. Plant-Microbe Interact. 23:1506-1513.
Koboldt, D. C., Chen, K. C., Wylie, T., Larson, D. E., McLellan, M. D., Mardis, E. R., Weinstock, G. M., Wilson, R. K., and Ding, L. 2009. VarScan: Variant detection in massively parallel sequencing of individual and pooled samples. Bioinformatics 25:2283-2285.
Konaté, G., Sarra, S., and Traoré, O. 2001. *Rice yellow mottle virus* is seed-borne but not seed transmitted in rice seeds. Eur. J. Plant Pathol. 107: 361-364.
Kouassi, N. K., N'Guessan, P., Albar, L., Fauquet, C., and Brugidou, C. 2005. Distribution and characterization of *Rice yellow mottle virus*: A threat to African farmers. Plant Dis. 89:124-133.
Lecoq, H., Moury, B., Desbiez, C., Palloix, A., and Pitrat, M. 2004. Durable virus resistance in plants through conventional approaches: A challenge. Virus Res. 100:31-39.
Li, H., and Durbin, R. 2010. Fast and accurate long-read alignment with Burrows-Wheeler transform. Bioinformatics 26:589-595.
Li, H., Handsaker, B., Wysoker, A., Fennell, T., Ruan, J., Homer, N., Marth, G., Abecasis, G., Durbin, R., and Subgroup, G. P. D. P. 2009. The sequence alignment/map (SAM) format and SAMtools. Bioinformatics 25:2078-2079.
Mariac, C., Scarcelli, N., Pouzadou, J., Barnaud, A., Billot, C., Faye, A., Kougbeadjo, A., Maillol, V., Martin, G., Sabot, F., Santoni, S., Vigouroux, Y., and Couvreur, T. 2014. Cost-effective enrichment hybridization capture of chloroplast genomes at deep multiplexing levels for population genetics and phylogeography studies. Mol. Ecol. Resour. 14:1103-1113.
Martin, M. 2011. Cutadapt removes adapter sequences from high-throughput sequencing reads. EMBnet.journal 17:10-12.
McKenna, A., Hanna, M., Banks, E., Sivachenko, A., Cibulskis, K., Kernytsky, A., Garimella, K., Altshuler, D., Gabriel, S., Daly, M., and DePristo, M. 2010. The Genome Analysis Toolkit: A MapReduce framework for analyzing next-generation DNA sequencing data. Genome Res. 20:1297-1303.
Ndjiondjop, M.-N., Albar, L., Sow, M., Yao, N., Djedatin, G., Thiemélé, D., and Ghesquière, A. 2013. Integration of molecular markers in rice improvement: A case study on resistance to *Rice yellow mottle virus*. Pages 161-172 in: Realizing Africa's Rice Promise. D. J. M. Wopereis, N. Ahmadi, E. Tollens, and A. Jalloh, eds. CABI, Cotonou, Benin.
Oludare, A., Tossou, H. T., Kini, K., and Silué, D. 2016. Diversity of *Rice yellow mottle virus* in Benin and Togo and screening for resistant accessions. J. Phytopathol. 164:924-935.
Pidon, H., Ghesquiere, A., Cheron, S., Issaka, S., Hebrard, E., Sabot, F., Kolade, O., Silue, D., and Albar, L. 2017. Fine mapping of RYMV3: A new resistance gene to *Rice yellow mottle virus* from *Oryza glaberrima*. Theor. Appl. Genet. 130:807-818.
Pinel-Galzi, A., Dubreuil-Tranchant, C., Hébrard, E., Mariac, C., Ghesquière, A., and Albar, L. 2016. Mutations in *Rice yellow mottle virus* polyprotein P2a involved in RYMV2 gene resistance breakdown. Front. Plant Sci. 7:1779.
Pinel-Galzi, A., Mpunami, A., Sangu, E., Rakotomalala, M., Traoré, O., Sérémé, D., Sorho, F., Séré, Y., Kanyeka, Z., Konaté, G., and Fargette, D. 2009. Recombination, selection and clock-like evolution of Rice yellow mottle virus. Virology. 394:164-172.
Pinel-Galzi, A., Rakotomalala, M., Sangu, E., Sorho, F., Kanyeka, Z., Traoré, O., Sérémé, D., Poulicard, N., Rabenantaondro, Y., Séré, Y., Konaté, G., Ghesquière, A., Hébrard, E., and Fargette, D. 2007. Theme and variations in the evolutionary pathways to virulence of an RNA plant virus species. PLoS Pathog. 3:e180.
Pinel-Galzi, A., Traoré, O., Séré, Y., Hébrard, E., and Fargette, D. 2015. The biogeography of viral emergence: *Rice yellow mottle virus* as a case study. Curr. Opin. Virol. 10:7-13.
Poulicard, N., Pinel-Galzi, A., Fargette, D., and Hebrard, E. 2014. Alternative mutational pathways, outside the VPg, of *Rice yellow mottle virus* to overcome eIF(iso)4G-mediated rice resistance under strong genetic constraints. J. Gen. Virol. 95:219-224.
Poulicard, N., Pinel-Galzi, A., Hébrard, E., and Fargette, D. 2010. Why *Rice yellow mottle virus*, a rapidly evolving RNA plant virus, is not efficient at breaking *rymv1-2* resistance. Mol. Plant Pathol. 11:145-154.
Poulicard, N., Pinel-Galzi, A., Traore, O., Vignols, F., Ghesquiere, A., Konate, G., Hebrard, E., and Fargette, D. 2012. Historical contingencies modulate the adaptability of *Rice yellow mottle virus*. PLoS Pathog. 8:e1002482.
Quenouille, J., Saint-Felix, L., Moury, B., and Palloix, A. 2016. Diversity of genetic backgrounds modulating the durability of a major resistance gene. Analysis of a core collection of pepper landraces resistant to Potato virus Y. Mol. Plant Pathol. 17:296-302.
Rakotomalala, M., Pinel-Galzi, A., Mpunami, A., Randrianasolo, A., Ramavovololona, P., Rabenantoandro, Y., and Fargette, D. 2013. *Rice yellow mottle virus* in Madagascar and in the Zanzibar Archipelago; island systems and evolutionary time scale to study virus emergence. Virus Res. 171:71-79.
Rozas, J., Sanchez-DelBarrio, J. C., Messeguer, X., and Rozas, R. 2003. DnaSP, DNA polymorphism analyses by the coalescent and other methods. Bioinformatics 19:2496-2497.
Séré, Y., Fargette, D., Abo, M. E., Wydra, K., Bimerew, M., Onasanya, A., and Akator, S. K. 2013. Managing the major diseases of rice in Africa. Pages 213-228 in: Realizing Africa's Rice Promise. M. C. S. Wopereis, D. E. Johnson, N. Ahmadi, E. Tollens, and A. Jalloh, eds. CABI, Cotonou, Benin.
Thiémélé, D., Boisnard, A., Ndjiondjop, M. N., Chéron, S., Séré, Y., Aké, S., Ghesquière, A., and Albar, L. 2010. Identification of a second major resistance gene to *Rice yellow mottle virus*, RYMV2, in the African cultivated rice species, *O. glaberrima*. Theor. Appl. Genet. 121:169-179.
Traoré, O., Pinel, A., Hébrard, E., Gumedzoé, M. Y. D., Fargette, D., Traoré, A. S., and Konaté, G. 2006a. Occurrence of resistance-breaking isolates of *Rice yellow mottle virus* in the West and Central Africa. Plant Dis. 90:259-263.
Traoré, O., Pinel-Galzi, A., Issaka, S., Poulicard, N., Aribi, J., Aké, S., Ghesquière, A., Séré, Y., Konaté, G., Hébrard, E., and Fargette, D. 2010. The adaptation of *Rice yellow mottle virus* to the eIF(iso)4G-mediated rice resistance. Virology 408:103-108.
Traoré, O., Sorho, F., Pinel, A., Abubakar, Z., Banwo, O., Maley, J., Hébrard, E., Winter, S., Séré, Y., Konaté, G., and Fargette, D. 2005. Processes of diversification and dispersion of *Rice yellow mottle virus* inferred from large-scale and high-resolution phylogeographical studies. Mol. Ecol. 14: 2097-2110.
Traoré, O., Traoré, M. D., Fargette, D., and Konaté, G. 2006b. Rice seedbeds as a source of primary infection by *Rice yellow mottle virus*. Eur. J. Plant Pathol. 115:181-186.
Traoré, V. S. E., Néya, B. J., Camara, M., Gracen, V., Offei, S. K., and Traore, O.. 2015. Farmers' perception and impact of Rice yellow mottle disease on rice yields in Burkina Faso. Agric. Sci. 6:943-952.
Trovão, N. S., Baele, G., Vrancken, B., Bielejec, F., Suchard, M. A., Fargette, D., and Lemey, P. 2015. Host ecology determines the dispersal patterns of a plant virus. Virus Evol. 1:vev016.